Transverse modulation instability of copropagating optical beams in nonlinear Kerr media

Govind P. Agrawal

The Institute of Optics, University of Rochester, Rochester, New York 14627

Received September 18, 1989; accepted January 17, 1990

Two optical beams, copropagating in a Kerr medium, interact with each other through cross-phase modulation. Such nonlinear beam coupling leads to a transverse modulation instability that is evident as spatial modulation of the beam profiles. A linear-stability analysis in the plane-wave approximation predicts the range of spatial frequencies over which modulation can occur. The case of self-defocusing media is particularly interesting, since modulation instability occurs only when both beams are present simultaneously. Numerical simulations are used to study how modulation instability can occur for finite-size beams. In particular, the mutual coupling of two copropagating Gaussian beams is studied in detail.

1. INTRODUCTION

Modulation instability generally refers to an instability of wave propagation in nonlinear dispersive media such that the steady state becomes unstable and evolves into a temporally modulated state.[1] In the context of nonlinear optics, modulation instability has been observed[2] in optical fibers. It generally leads to the breakup of a cw or quasi-cw beam into a periodic pulse train. The concept of transverse modulation instability originates from a space–time analogy that exists when dispersion is replaced by diffraction.[3] In this case a cw optical beam is spatially modulated along the transverse dimensions as a result of the combined effects of nonlinearity and diffraction. Indeed, the well-known instability of a plane wave in a self-focusing Kerr medium[4] is an example of transverse modulation instability. Similarly, self-trapping[5] and filamentation[6] of optical beams can be interpreted in terms of the solitary-wave solutions of the nonlinear wave equation.

Recently the phenomenon of cross-phase modulation (XPM) has attracted considerable attention in the context of optical fibers in which the XPM interaction between the two copropagating optical pulses leads to interesting new effects.[7,8] Following the space–time analogy, one would expect the XPM interaction between the two copropagating optical beams to give rise to novel transverse effects manifested through spatial modifications of the beam profiles. The objective of this paper is to study such XPM-induced transverse modulation instabilities for the case in which two optical beams at different wavelengths are launched into a nonlinear Kerr medium. Similar transverse modulation instabilities are predicted to occur in the case of counterpropagating optical beams.[9] In this paper the focus is on the case of copropagating beams exclusively.

The paper is organized as follows. The coupled amplitude equations are obtained in Section 2. These equations include the effects of diffraction, self-phase modulation (SPM), and XPM. The stability of the plane-wave solution of these equations is examined in Section 3 by using a linear-stability analysis. Section 4 extends the analysis beyond the plane-wave approximation by solving the coupled amplitude equations numerically for the Gaussian beams. One of the beams is intense and the other much less intense in the pump–probe configuration considered in Section 4. The case of two intense beams is discussed in Section 5. The results are summarized in Section 6.

2. COUPLED AMPLITUDE EQUATIONS

The refractive index of a nonlinear Kerr medium can be written in the form

$$n = n_0 + 2n_2|\mathbf{E}|^2, \tag{1}$$

where n_0 is the linear part of the refractive index and n_2 is the Kerr coefficient responsible for the nonlinearity. If we assume that the two copropagating beams at the frequencies ω_1 and ω_2 are linearly polarized, then the electric field $\mathbf{E}(\mathbf{r}, t)$ can be written in the form

$$\mathbf{E}(\mathbf{r}, t) = \frac{1}{2}\hat{x}\sum_{j=1}^{2} A_j(\mathbf{r}, t)\exp[i(k_j z - \omega_j t)] + \text{c.c.}, \tag{2}$$

where $\hat{x}$ is the polarization unit vector and the wave number is

$$k_j = n_{0j}\omega_j/c = 2\pi n_{0j}/\lambda_j. \tag{3}$$

The linear refractive index $[n_{0j} = n_0(\omega_j)]$ is generally different for the two beams because of the frequency dependence of n_j that results from chromatic dispersion. The frequency dependence of n_2 is ignored by assuming that it does not change significantly in the frequency range $|\omega_1-\omega_2|$. Its inclusion, if necessary, is straightforward.

The coupled amplitude equations describing propagation of the two optical beams are obtained by substituting Eqs. (1) and (2) into the wave equation. If we assume cw or quasi-cw beams and make the paraxial approximation, the coupled amplitude equations take the form

$$\frac{\partial A_1}{\partial z} - \frac{i}{2k_1}\left(\frac{\partial^2 A_1}{\partial x^2} + \frac{\partial^2 A_1}{\partial y^2}\right) = \frac{ik_1 n_2}{n_{01}}(|A_1|^2 + 2|A_2|^2)A_1, \tag{4}$$

0740-3224/90/061072-07$02.00

$$\frac{\partial A_2}{\partial z} - \frac{i}{2k_2}\left(\frac{\partial^2 A_2}{\partial x^2} + \frac{\partial^2 A_2}{\partial y^2}\right) = \frac{ik_2 n_2}{n_{02}}(|A_2|^2 + 2|A_1|^2)A_2. \quad (5)$$

The two terms on the right-hand sides of these equations account for SPM and XPM imposed on each beam by the Kerr nonlinearity. These equations are similar to those describing pulse propagation in optical fibers,[7] in which the transverse Laplacian (describing diffraction along x and y) is replaced by a dispersion term containing $\partial_2 A_j/\partial t^2$ for $j = 1$ and $j = 2$. This extra degree of freedom associated with beam diffraction makes the numerical solution of Eqs. (4) and (5) a more demanding task.

3. TRANSVERSE MODULATION INSTABILITY

The origin of transverse modulation instability is most clearly seen when the incident waves are assumed to be plane waves of constant intensities I_1 and I_2, i.e.,

$$A_j(x, y, 0) = \sqrt{I_j}, \qquad j = 1, 2. \quad (6)$$

Equations (4) and (5) are readily solved in this specific case, and the solution is

$$\bar{A}_j(x, y, z) = \sqrt{I_j}\exp\left[ik_j z\frac{n_2}{n_{0j}}(I_j + 2I_{3-j})\right], \quad (7)$$

where $j = 1$ or $j = 2$. Thus a plane wave remains unchanged on propagation except for acquiring an intensity-dependent phase. The stability of the solution [Eq. (7)] is examined by performing a linear-stability analysis. Since the procedure is well known,[10-12] it is described only briefly. Assume that the steady state is perturbed such that

$$A_j = \bar{A}_j \times \{1 + u_j(z)\exp[i(px + qy)] + v_j^*(z)\exp[-i(px + qy)]\}, \quad (8)$$

where p and q are the components of the spatial frequency S ($S^2 = p^2 + q^2$) associated with the transverse perturbation. Substitute Eq. (8) into Eqs. (4) and (5) and linearize in u_1, u_2, v_1^*, and v_2^*. The resulting set of equations has a nontrivial solution of the form $u_j \sim \exp(iKz)$, where K is the wave number. The perturbation grows exponentially whenever K has a negative imaginary part, and the corresponding plane-wave solution [Eq. (7)] is then unstable. The wave number K is determined by the dispersion relation[11]

$$(K^2 - h_1^2)(K^2 - h_2^2) = C^2, \quad (9)$$

where

$$h_j = (S/2k_j)[S^2 - \mathrm{sgn}(n_2)S_{cj}^2]^{1/2}, \quad (10)$$

$$C = S^2\left(\frac{S_{c1}S_{c2}}{k_1 k_2}\right), \quad (11)$$

and S_{cj} is a critical spatial frequency defined by

$$S_{cj} = 2k_j(|n_2|I_j/n_{0j})^{1/2}, \qquad j = 1, 2 \quad (12)$$

in terms of the nonlinear index change $n_2 I_j$ induced by each beam.

The dispersion relation [Eq. (9)] shows that K becomes imaginary whenever $C > h_1 h_2$. This is the necessary condition for transverse modulation instability. By using Eqs. (10) and (11) the instability condition can be written in the form

$$[S^2 - \mathrm{sgn}(n_2)S_{c1}^2][S^2 - \mathrm{sgn}(n_2)S_{c2}^2] < 4S_{c1}^2 S_{c2}^2. \quad (13)$$

Thus the plane-wave solution is unstable against perturbations whose spatial frequency S satisfies Eq. (13). The range of unstable S depends not only on the beam intensities I_1 and I_2 through Eq. (12) but also on the sign of the Kerr coefficient n_2. This is shown in Fig. 1, where the modulation-instability gain $g = 2\,\mathrm{Im}(K)$ is plotted as a function of S for the case of two equal-intensity beams at wavelengths 0.53 and 0.6 μm. The beam intensities are such that the nonlinear index change $\Delta n = n_2 I_1 = 1 \times 10^{-6}$. The linear refractive index $n_{01} \simeq n_{02} = 1.5$. In general, both the gain and the frequency range are smaller for a self-defocusing medium ($n_2 < 0$). This is not surprising if we note that a plane wave, when propagating alone, is stable in a self-defocusing medium. However, the plane wave becomes unstable if it propagates together with another plane wave of a different wavelength. The origin of instability is related to the XPM-induced coupling between the two waves.[10-12] This can be seen clearly in Eq. (9) after noting that $C = 0$ in the absence of XPM-induced coupling. Note also from Eq. (13) that modulation instability would not occur in the defocusing case if the XPM contribution in Eqs. (4) and (5) appeared with a coefficient 1 rather than 2. Physically, nonlinear nonreciprocity plays an essential role in destabilizing the plane-wave propagation in self-defocusing media.

Figure 1 shows that the modulation-instability gain of $\sim$1 cm^{-1} is possible at a spatial frequency $\sim$400 cm^{-1} for a beam intensity such that $n_2 I_1 = 10^{-6}$. Thus the two beams can develop spatial modulation with a period $2\pi/S \sim 100$ μm over a propagation length of $\sim$10 cm through noise amplification. Both the modulation period and the needed propagation length decrease for more intense input beams.

4. PUMP-PROBE CONFIGURATION

The preceding linear-stability analysis shows that when two optical beams that are copropagating in a Kerr medium

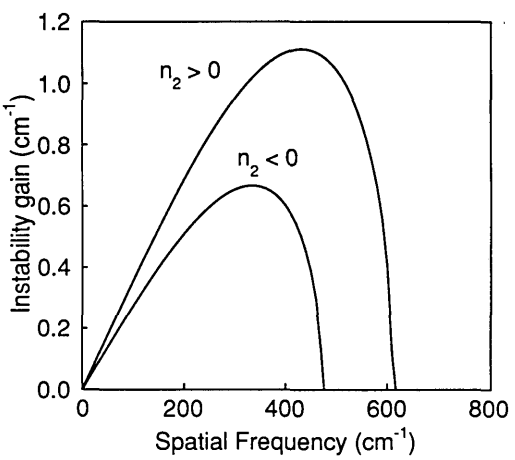

Fig. 1. Modulation instability gain versus spatial frequency S for the self-focusing ($n_2 > 0$) and self-defocusing ($n_2 < 0$) cases when two plane waves of equal intensities such that $\Delta n = n_2 I = 10^{-6}$ copropagate inside the nonlinear medium.

interact with each other through XPM they are likely to develop spatial modulation as a result of transverse modulation instability. The analysis is, however, performed in the plane-wave approximation, whereas the optical beams, in practice, are limited in their transverse extent. In this section I consider the case of two copropagating Gaussian beams in order to model the practical situation more realistically. In particular, I consider a pump–probe configuration in which a low-intensity probe beam is copropagated with an intense pump wave. The objective is to study how the near and far fields of the probe beam are affected by the presence of the copropagating pump wave.

The pump–probe interaction is governed by the coupled amplitude equations (4) and (5) that were obtained in Section 2. As mentioned there, numerical solution of these equations require considerable computing resources when both x and y derivatives are included. For simplicity, diffractive transverse coupling is limited to one dimension by setting $\partial A_j/\partial y = 0$ for $j = 1$ and $j = 2$. Although this approximation is commonly made in treating transverse modulation instabilities,[9] one must be aware of its limitations and interpret the results with caution. For the purpose of numerical computations, the normalized variables

$$X = \frac{x}{w_0}, \qquad \xi = \frac{z}{L_D}, \qquad U_j = \frac{A_j}{(I_1)^{1/2}} \tag{14}$$

are also introduced. Equations (4) and (5) then take the form

$$\frac{\partial U_1}{\partial \xi} - \frac{i}{2}\frac{\partial^2 U_1}{\partial X^2} = \mathrm{sgn}(n_2) iN^2(|U_1|^2 + 2|U_2|^2)U_1, \tag{15}$$

$$\frac{\partial U_2}{\partial \xi} - \frac{i}{2}\frac{\lambda_2}{\lambda_1}\frac{\partial^2 U_2}{\partial X^2} = \mathrm{sgn}(n_2)\frac{\lambda_1}{\lambda_2} iN^2(|U_2|^2 + 2|U_1|^2)U_2, \tag{16}$$

where λ_2/λ_1 is the probe-to-pump wavelength ratio and it is assumed that $n_{01} \simeq n_{02}$. The nonlinear interaction is described in terms of a single parameter N, defined by

$$N^2 = L_D(k_1/n_{01})n_2 I_1 = k_1{}^2 w_0{}^2(|n_2|I_1/n_{01}), \tag{17}$$

where $L_D = k_1 w_0{}^2$ is the diffraction length (also known as the Rayleigh length) and w_0 is related to the pump-beam spot size. In the visible region ($\lambda_1 \sim 0.5\,\mu$m), $L_D \sim 10$ cm and $N \sim 1$ for $w_0 = 100\,\mu$m and $|n_2|I_1 \sim 10^{-6}$.

Equations (15) and (16) are solved numerically by using the split-step Fourier method.[13] The initial field distribution at $\xi = 0$ depends on the spatial profile of the two beams. If we assume that the pump and the probe beams are Gaussian with the $1/e$ half-widths w_0 and w_0', respectively, we have

$$U_1(0, X) = \exp(-X^2/2), \tag{18}$$

$$U_2(0, X) = (I_2/I_1)^{1/2}\exp\left[-\left(\frac{w_0'}{w_0}\right)^2\frac{X^2}{2}\right]. \tag{19}$$

It is implicitly assumed that the beam centers coincide exactly. This need not be the case in general. In the following discussion it is assumed that $w_0 = w_0'$. The pump intensity is chosen such that the parameter $N = 10$ [see Eq. (17)]. The probe intensity is chosen to be very small ($I_2/I_1 = 10^{-4}$). The only other parameter that needs to be specified is the wavelength ratio, which is chosen to be $\lambda_2/\lambda_1 = 0.9$. The numerical solution of Eqs. (15) and (16) provides the complex field distributions $U_1(\xi, X)$ and $U_2(\xi, X)$. The near field is given by $|U_j(\xi, X)|^2$, while the Fourier transform of $U_j(\xi, X)$ provides the far field ($j = 1$ or $j = 2$). The far-field intensity can be written as

$$I_j^{\mathrm{FF}}(p) = \left|\int_{-\infty}^{\infty} U_j(L, X)\exp(2\pi i p X)\mathrm{d}X\right|^2, \tag{20}$$

where the Fourier variable p is related to the far-field angle θ by $p = (w_0/\lambda_1)\sin\theta$ and L is the length of the Kerr medium. Equation (20) can also be thought to provide the angular spectrum or the Fourier spectrum with respect to the spatial frequency $S = 2\pi p/w_0$.

Let us first consider the case of a self-defocusing medium by choosing $\mathrm{sgn}(n_2) = -1$ in Eqs. (15) and (16). This case in interesting, since the transverse modulation instability does

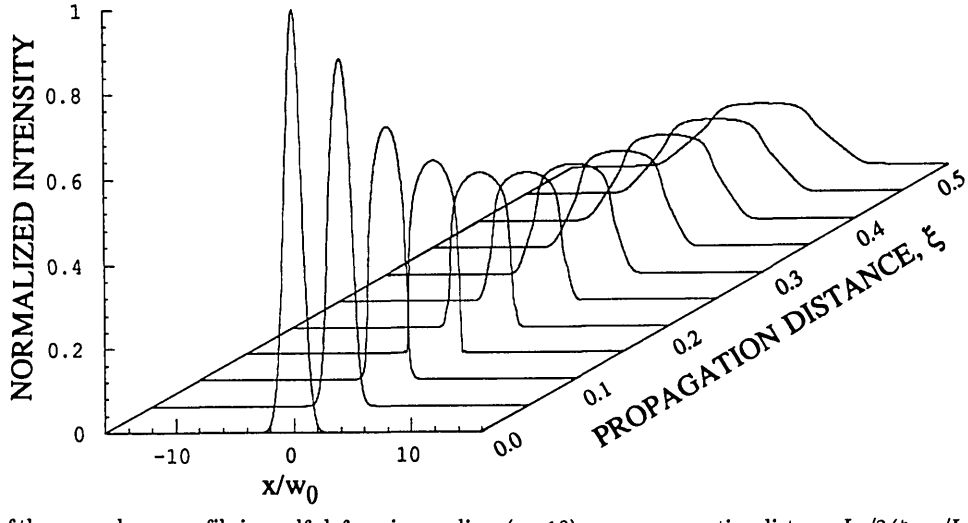

Fig. 2. Evolution of the pump-beam profile in a self-defocusing medium ($n_2 < 0$) over a propagation distance $L_D/2$ ($\xi = z/L_D$). The input beam is Gaussian with a peak intensity such that $N = 10$.

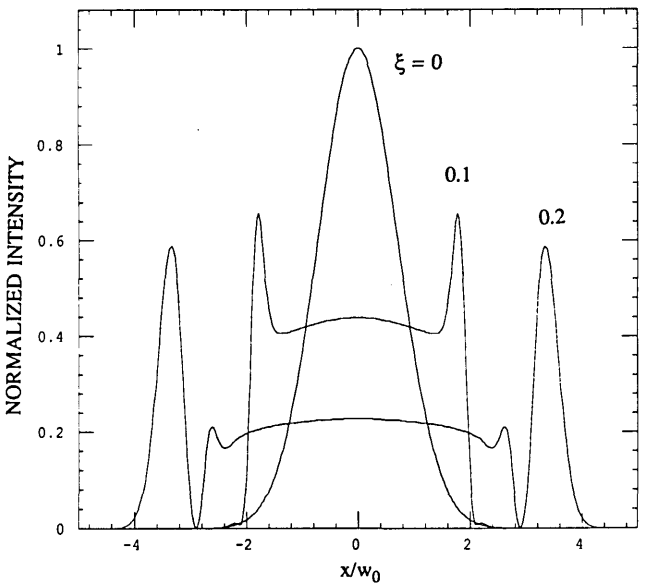

Fig. 3. Probe-beam profiles at $\xi = 0.1$ and $\xi = 0.2$ in a self-focusing medium ($n_2 < 0$). The input Gaussian profile at $\xi = 0$ is also shown for comparison. The probe beam is launched together with a Gaussian pump beam whose peak intensity corresponds to $N = 10$.

not occur when each beam propagates by itself. Because the probe beam is too weak to influence the pump beam, the latter is expected to defocus as it propagates inside the Kerr medium. This behavior is evident in Fig. 2, where the evolution of the pump-beam profile is shown over a range ξ equal to 0–0.5. The probe beam, on the other hand, is strongly affected by the presence of the pump beam. This is seen in Fig. 3, where the probe-beam profiles are shown at $\xi = 0.1$ and $\xi = 0.2$ and are compared with the input Gaussian profile at $\xi = 0$. The probe beam defocuses, as one would expect. However, its coupling with the pump beam through XPM also leads to spatial modulation of the beam profile. In the three-dimensional case the modulated profile would correspond to a ring pattern. The number of rings increases with further propagation. Figure 4 compares the beam profile at $\xi = 0.5$ with the input Gaussian profile. The probe beam has defocused considerably and exhibits three rings near its edges.

In many experimental situations the probe beam is characterized through far-field measurements. The far field contains information about the phase front associated with the near-field profile and can be obtained by taking the Fourier transform indicated in Eq. (20). Figure 5 shows the far field that corresponds to the near field shown in Fig. 4. A ring pattern is predicted, with the two outermost rings to be the most intense. The changes seen in both the near and far fields are a consequence of XPM-induced coupling between the pump and the probe beams.

The self-focusing case, in which the pump and the probe beams interact with each other in a medium with positive n_2, is briefly considered. The parameter values are identical to those used before. In particular, $N = 10$, $I_2/I_1 = 10^{-4}$, and $\lambda_2/\lambda_1 = 0.9$. The probe intensity is below the self-focusing threshold. Thus the probe is expected to diffract in the absence of the pump. However, the XPM interaction with the pump can induce focusing of the probe.[14,15] This behavior is shown in Fig. 6, where the probe-beam profile at $\xi = 0.05$ is shown and compared with the input Gaussian profile. Both the pump and the probe beams develop high-frequency spatial modulation beyond $\xi > 0.1$. These modulations result from self-focusing and filamentation of the pump beam that are expected to occur even in the absence of the probe beam. Although Fig. 6 was obtained by considering only one transverse dimension, induced focusing has been predicted to occur when both transverse dimensions are included.[14] It has also been observed in an experiment[15] in which Stokes radiation from stimulated Raman scattering that occurred in a multimode fiber was found to be focused as a result of the pump-induced XPM.

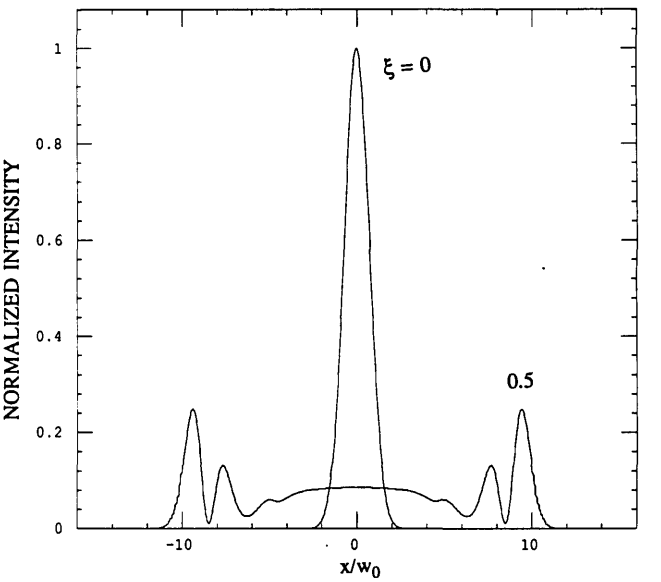

Fig. 4. Same as in Fig. 3 except that the probe-beam profile at $\xi = 0.5$ is compared with the input Gaussian profile.

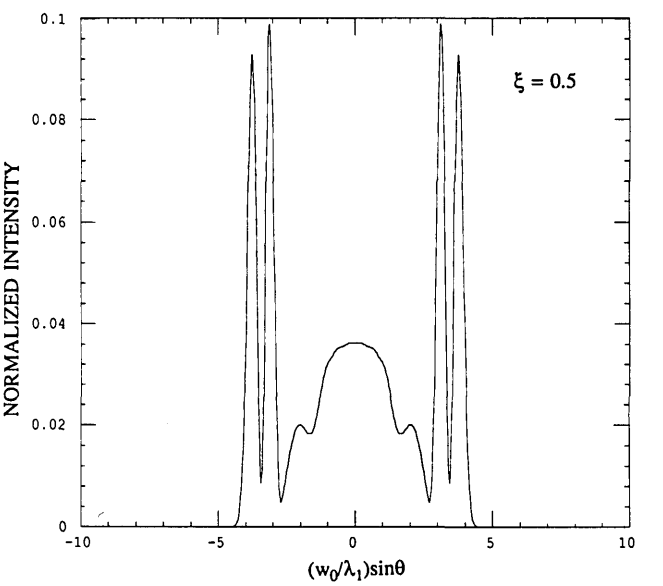

Fig. 5. Far-field intensity versus diffraction angle θ. The corresponding near field is shown in Fig. 4 at $\xi = 0.5$.

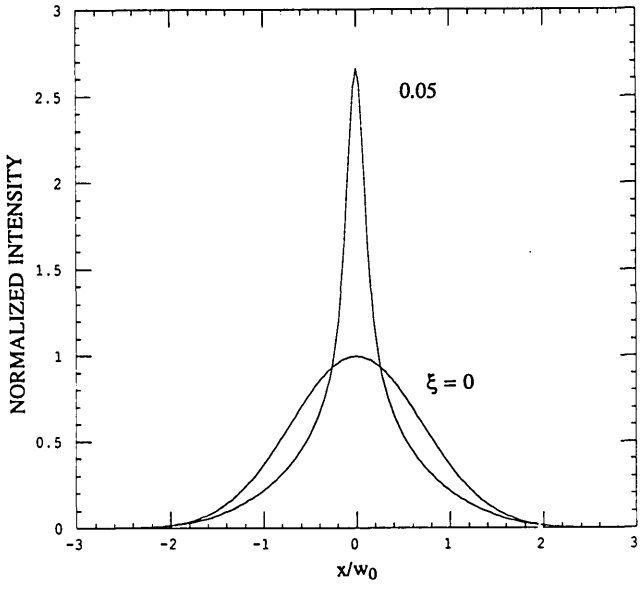

Fig. 6. Induced focusing of a probe beam copropagated with an intense pump beam ($N = 10$) in a self-focusing medium ($n_2 > 0$). The probe-beam profile at $\xi = 0.05$ is compared with the input Gaussian profile. The probe peak intensity is much below the self-focusing threshold.

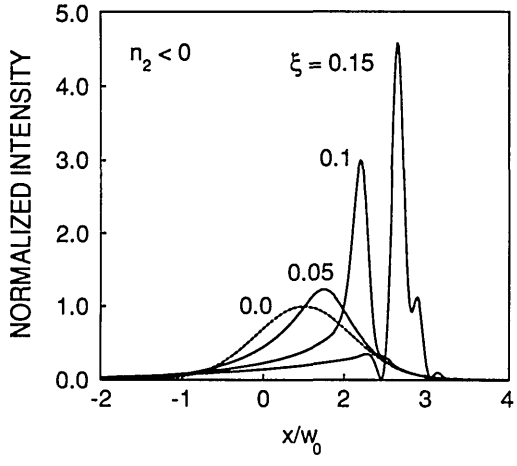

Fig. 7. Probe beams profiles showing pump-induced focusing in a self-defocusing medium ($n_2 < 0$). The input profile at $\xi = 0$ peaks at $x = w_0$, whereas the pump-beam profile peaks at $x = 0$. Other parameters are identical to those used for Fig. 6.

Induced focusing of the probe beam can occur even in self-defocusing media. Although counterintuitive, this phenomenon is possible when the pump and probe profiles are displaced with respect to each other so that they overlap only partially. Figure 7 shows the probe profiles obtained by using parameter values identical to those of Fig. 6 except that n_2 is assumed to be negative (self-defocusing medium) and that the probe intensity peaks at $x = w_0$ while the pump intensity peaks at $x = 0$. The pump beam defocuses and follows the pattern of evolution shown in Fig. 2. By contrast, the probe beam evolves in the manner shown in Fig. 7. A part of the probe power (contained in the region $x < w_0$) defocuses, whereas the other part contained in the region $x > w_0$ begins to focus and forms a narrow peak centered near $x = 2w_0$. The full width at half-maximum of the narrow peak is smaller than the input-beam width by approximately a factor of 8 for ξ in the range 0.1–0.15. For larger values of ξ the probe-beam profile splits into two components whose widths increase with ξ. The physical mechanism behind induced focusing for $\xi \leq 0.15$ is XPM. In particular, the pump contribution to the probe phase produces a locally converging phase front. It is important to note that this behavior is quite different from that shown in Fig. 6, where the whole beam appears to be focusing.[14]

5. INTENSE BEAMS

In the pump–probe configuration discussed in Section 4, the spatial frequency of probe modulation is rather small. This can be understood from Eq. (9) by noting that the coupling parameter C depends on $(I_1 I_2)^{1/2}$. In this section the case of two intense copropagating beams is considered, and the development of transverse modulation instability is studied. As before, Eqs. (15) and (16) are solved with the initial conditions of Eqs. (18) and (19), except that the input beam intensities are now taken to be equal ($I_1 = I_2$). For comparison we assume a self-defocusing medium ($n_2 < 0$) and still use the same parameter values $N = 10$ and $\lambda_2/\lambda_1 = 0.9$. Figures 8 and 9 show the near- and far-field profiles for beam 1 and beam 2, respectively, at $\xi = 0.1$ (top) and $\xi = 0.2$ (bottom). Differences in the Figs. 8 and 9 are entirely due to different wavelengths of the otherwise identical input beams. Input profiles for both beams are Gaussian. At $\xi = 0.1$ the beam profiles, although far from Gaussian, are still nearly smooth. The beam profiles develop rapid modulations at $\xi = 0.2$ as a result of transverse modulation instability.

The plane-wave theory of Section 3 can be used to understand the main features qualitatively. The XPM-induced coupling between the two waves implies that perturbations with spatial frequencies $S < S_{cj}$ are unstable and would amplify exponentially ($j = 1, 2$). The far-field patterns or the angular spectra shown on the right-hand sides of Figs. 8 and 9 show the range of spatial frequencies associated with each beam. At $\xi = 0.1$ the angular spectrum is considerably broader than the input spectrum as a result of the combined effects of SPM and XPM and exhibits a characteristic multipeak profile. Its frequency range, however, is not large enough to initiate modulation instability. For $\xi > 0.1$ the angular spectrum becomes smoother as diffraction becomes more and more important and mixes various peaks. The spectrum also becomes wider as SPM and XPM continue to broaden it. When the spectral width becomes comparable to S_{cj}, modulation instability begins to amplify spatial frequencies in the vicinity of S_{cj}. As a result, the beam profile becomes modulated at such frequencies. The fact that spatial modulation is accompanied by the growth of spatial frequencies in the vicinity of S_{cj} is evident in Fig. 9. In fact, the location of the side peaks in the far-field profile agrees approximately with the prediction of Eq. (12). These numerical results show that the instability predicted by the plane-wave analysis can be observed even by using Gaussian beams as long as the input beam radius is much larger than the modulation period. It should be stressed that no initial modulation was imposed on the input Gaussian beams. The instability gain is high enough that modulation can grow within a relatively short propagation distance from amplification of the unstable spatial-frequency component generated by SPM and XPM.

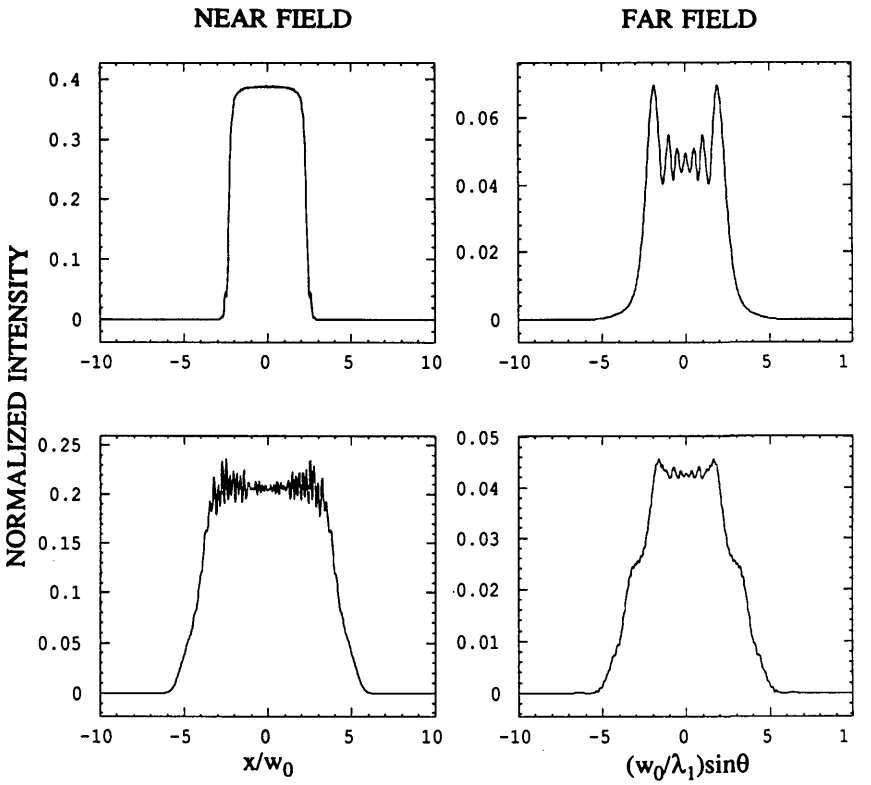

Fig. 8. Near- and far-field profiles of an optical beam copropagating with another equally intense beam in a self-defocusing medium. The top and bottom rows correspond to $\xi = 0.1$ and $\xi = 0.2$, respectively. High-frequency modulation of the near-field profile at $\xi = 0.2$ is due to the onset of the transverse modulation instability.

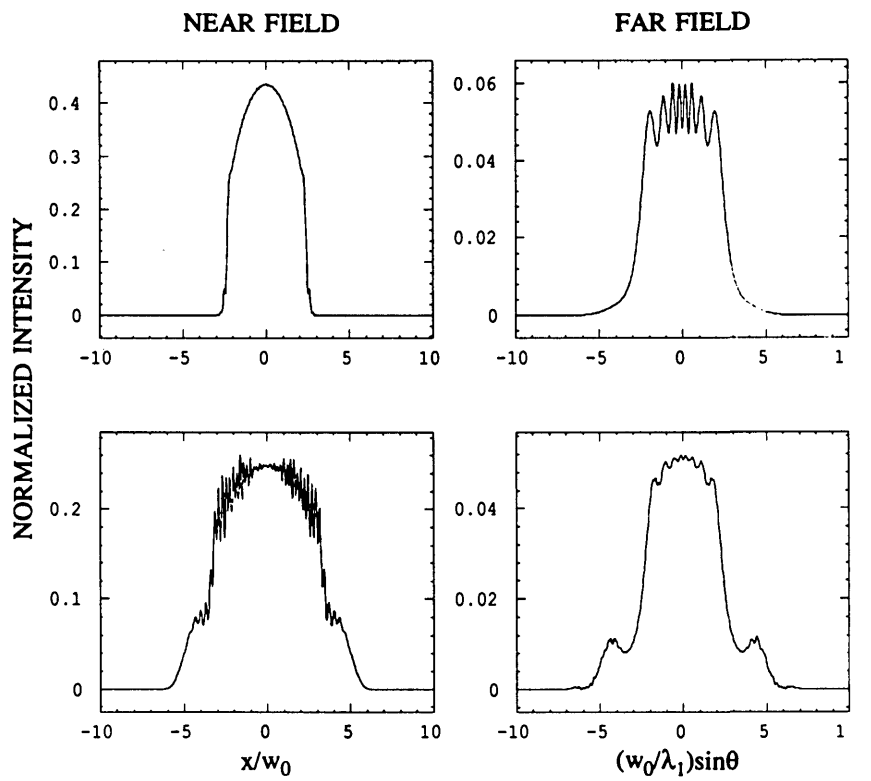

Fig. 9. Same as in Fig. 8 except that the near- and far-field profiles of the second beam are shown. The differences in Figs. 8 and 9 are entirely due to the lower wavelength ($\lambda_2/\lambda_1 = 0.9$) of the second beam. The side peaks in the far-field profile at $\xi = 0.2$ are due to the onset of the transverse modulation instability.

6. DISCUSSION AND CONCLUSION

In this paper mutual coupling of two copropagating optical beams (at different wavelengths), occurring as a result of XPM in nonlinear Kerr media, was discussed. Such a coupling leads to an instability, referred to here as a transverse modulation instability, that is evident through spatial modulations of the beam profiles. In the case of a self-focusing medium with positive n_2, the instability exists even when each beam propagates alone in the medium; the role of XPM-induced coupling is to enhance the gain and the frequency range over which the instability can occur. By contrast, when the beams propagate in a self-defocusing medium with negative n_2, the instability is due solely to XPM-induced coupling, since each beam is stable in isolation. The origin and the main features of transverse modulation instability have been discussed in the plane-wave approximation by performing a linear-stability analysis.

The case of finite-size beams is considered by solving the coupled-amplitude equations numerically. The spatial profile of each beam is found to be modulated as a result of transverse modulation instability. These transverse effects should be observable experimentally. An order-of-magnitude estimate shows a modulation period of $\sim 100\ \mu$m for the beam intensities such that the nonlinear index change is $|n_2|I \sim 10^{-6}$. In general, XPM provides a way through which a weak probe beam can be manipulated in a Kerr medium by copropagating it with a strong pump beam. As an example, it was shown in Section 4 that the probe beam can exhibit induced focusing in a medium with positive n_2 even though its intensity is well below the critical power for self-trapping. It was also found that under certain conditions induced focusing of the probe can occur even in a self-defocusing medium.

ACKNOWLEDGMENTS

It is a pleasure to acknowledge stimulating discussions with R. W. Boyd and C. J. McKinstrie. This research was partially supported by the Joint Services Optics Program and the U.S. Army Research Office.

REFERENCES

1. For a recent review, see G. P. Agrawal, *Nonlinear Fiber Optics* (Academic, Boston, Mass., 1989), Sec. 5.1.
2. K. Tai, A. Hasegawa, and A. Tomita, Phys. Rev. Lett. **56,** 135 (1986).
3. S. A. Akhmanov, V. A. Vysloukh, and A. S. Chirkin, Sov. Phys. Usp. **29,** 642 (1986).
4. V. I. Bespalov and V. I. Talanov, JETP Lett. **3,** 307 (1966).
5. R. Y. Chiao, E. Garmire, and C. H. Townes, Phys. Rev. Lett. **13,** 479 (1964).
6. E. Garmire, R. Y. Chiao, and C. H. Townes, Phys. Rev. Lett. **16,** 347 (1966).
7. G. P. Agrawal, *Nonlinear Fiber Optics* (Academic, Boston, Mass., 1989), Chap. 7.
8. P. L. Baldeck, P. P. Ho, and R. R. Alfano, in *The Supercontinuum Laser Source,* R. R. Alfano, ed. (Springer-Verlag, New York, 1989), Chap. 4.
9. W. J. Firth and C. Paré, Opt. Lett. **13,** 1096 (1988).
10. G. P. Agrawal, Phys. Rev. Lett. **59,** 880 (1987).
11. G. P. Agrawal, P. L. Baldeck, and R. R. Alfano, Phys. Rev. A **39,** 3406 (1989).
12. C. J. McKinstrie and R. Bingham, Phys. Fluids B **1,** 230 (1989).
13. See, for example, Sec. 2.4 of Ref. 7.
14. C. J. McKinstrie and D. A. Russell, Phys. Rev. Lett. **61,** 2929 (1988).
15. P. L. Baldeck, F. Raccah, and R. R. Alfano, Opt. Lett. **12,** 588 (1987).